

Catalytic Deoxygenation of Nitroarenes Mediated by High-Valent Molybdenum(VI)–NHC Complexes

Shenyu Liu, Jorge Ivan Amaro-Estrada, Marc Baltrun, Iskander Douair, Roland Schoch, Laurent Maron,* and Stephan Hohloch*



Cite This: *Organometallics* 2021, 40, 107–118



Read Online

ACCESS |



Metrics & More

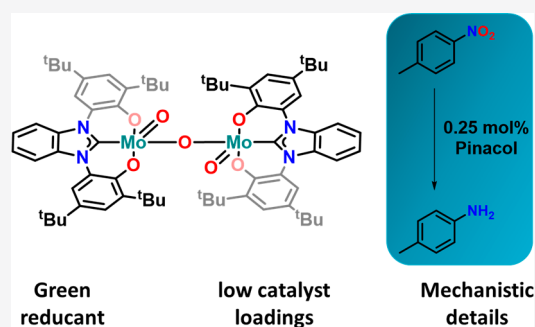


Article Recommendations



Supporting Information

ABSTRACT: The high-valent molybdenum(VI) N-heterocyclic carbene complexes, (NHC)MoO₂ (**1**) and (NHC)MoO(N^tBu) (**2**) (NHC = 1,3-bis(3,5-di-*tert*-butyl-2-phenolato)-benzimidazol-2-ylidene), are investigated toward their catalytic potential in the deoxygenation of nitroarenes. Using pinacol as the sacrificial and green reductant, both complexes are shown to be very active (pre)catalysts for this transformation allowing a reduction of the catalyst loading down to 0.25 mol %. Mechanistic investigations show μ -oxo bridged molybdenum(V) complexes [(NHC)MoO]₂O (**4**) and [(NHC)Mo(N^tBu)]₂O (**5**) as well as zwitterionic pinacolate benzimidazolium complex **6**, with a doubly protonated NHC ligand, to be potentially active species in the catalytic cycle. Both **4** and **5** can be prepared independently by the deoxygenation of **1** and **2** using triethyl phosphine (PEt₃) or triphenyl phosphine (PPh₃) and were shown to exhibit an unusual multireferenced ground state with a very small singlet–triplet gap at room temperature. Computational studies show that the spin state plays an unneglectable role in the catalytic process, efficiently lowering the reaction barrier of the deoxygenation step. Mechanistic details, putting special emphasis on the fate of the catalyst will be presented and potential routes how nitroarene reduction is facilitated are evaluated.

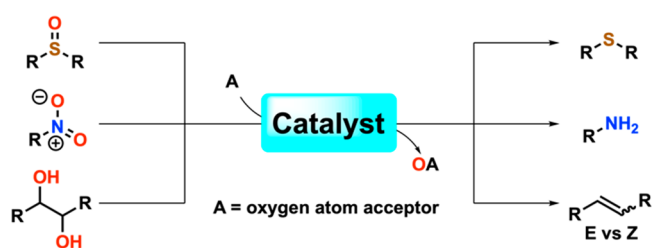


INTRODUCTION

The development of new catalytic systems that can promote the reduction of oxidatively over functionalized molecules under environmentally benign and economic conditions is one of the key targets in industrial and academic research.^{1,2} Despite many achievements have already been realized in this area,^{3–5} the search for milder reaction conditions, the reduction of the catalyst loading, or the avoidance of precious metal catalysts, as well as pressurized reactors, still remain important goals.

While traditional methods such as direct hydrogenation^{6–9} or transfer hydrogenation¹⁰ have been intensively explored in this area, these methods still have some major drawbacks, as the need for precious metal catalysts,^{4,11–15} complicated (chemo-)selectivity strategies,^{16–20} or the need for pressurized reactors, which are not commonly available in all laboratories, as well as the need for potentially hazardous hydrogen gas.²¹ Although the latter can be overcome by using transfer hydrogenation processes^{14–16,22–24} with different hydrogen delivering reagents, e.g., isopropanol or silanes, these protocols often require a large excess of hydrogen suppliers and may create large amounts of (hazardous) waste byproducts.^{13,25–28} In this context, oxygen atom transfer reactions (OATR, Scheme 1) hold great promise, not only because of their high atom efficiency^{29–33} but also due to simple executions and the need for cheap, earth-abundant early transition metals.^{34–36}

Scheme 1. Generalized Scheme of the Deoxygenation of Sulfoxides, Nitroarenes, and Vicinal Diols by Oxygen Atom Transfer Catalysis

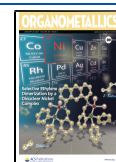


Furthermore, OAT reactions focus only on oxygen containing functional groups, which makes them ideal candidates for chemoselective reductions compared to “classical” hydrogenation reactions.

Prominent candidates facilitating oxygen atom transfer catalysis (OATC) are high-valent molybdenum complexes as

Received: May 20, 2020

Published: January 4, 2021



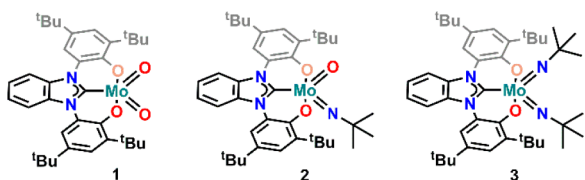


Figure 1. Overview of high-valent Mo-NHC complexes recently reported by our group.

this element combines three advantages: (i) It is environmentally friendly and earth abundant,³⁷ (ii) it is relatively cheap compared to many other 4d metals^{37–39} and (iii) it is capable of binding oxygen reversibly. Thus, complexes of the general formula $\text{MoO}_2\text{Cl}_2(\text{L})_2$ ($\text{L} = \text{DMF}$, DPPE , and DME) have recently been shown to be prominent catalysts for the deoxygenation of sulfoxides, phosphine oxides, and N-oxides, including nitroarenes.^{5,40–45} However, one major drawback of these systems is that although molybdenum is an environmentally friendly metal a large amount of catalyst (between 5 and 10 mol %) ^{46,47} is still necessary to efficiently perform OATC, especially for the reduction of nitroarenes to anilines.⁵

One strategy that has been successfully employed in the past years to reduce catalyst loadings and enhance the catalytic potential of metal complexes is the introduction of one or more *N*-heterocyclic carbene (NHC) ligands.^{48–54} Despite high-valent molybdenum(VI)-oxo NHC complexes having been found to be rare and lack stability,^{55–58} Buchmeiser and co-workers have shown that NHC ligands are indeed valuable supporting ligands in high-valent molybdenum- and tungsten-catalyzed metathesis reactions.^{59–67} Closing the gap for dioxo, oxo-imido, and bis-imido molybdenum complexes we have recently discovered the facile and simple synthesis of a series of high-valent molybdenum(VI) NHC complexes 1–3 (compare Figure 1)^{68,69} taking advantage of anionic tethered NHC-ligands,^{70–79} using a pincer-type OCO-benzimidazolyli-dene ligand originally introduced by Bellemin-Laponnaz and Bercaw.^{80–82}

Herein, we will evaluate the catalytic potential of 1 and 2 in the OATC converting nitroarenes into anilines using pinacol as a green and environmentally friendly reductant. Deoxygenation of 1 and 2 yields the oxo-bridged dimers 4 and 5, via a putative

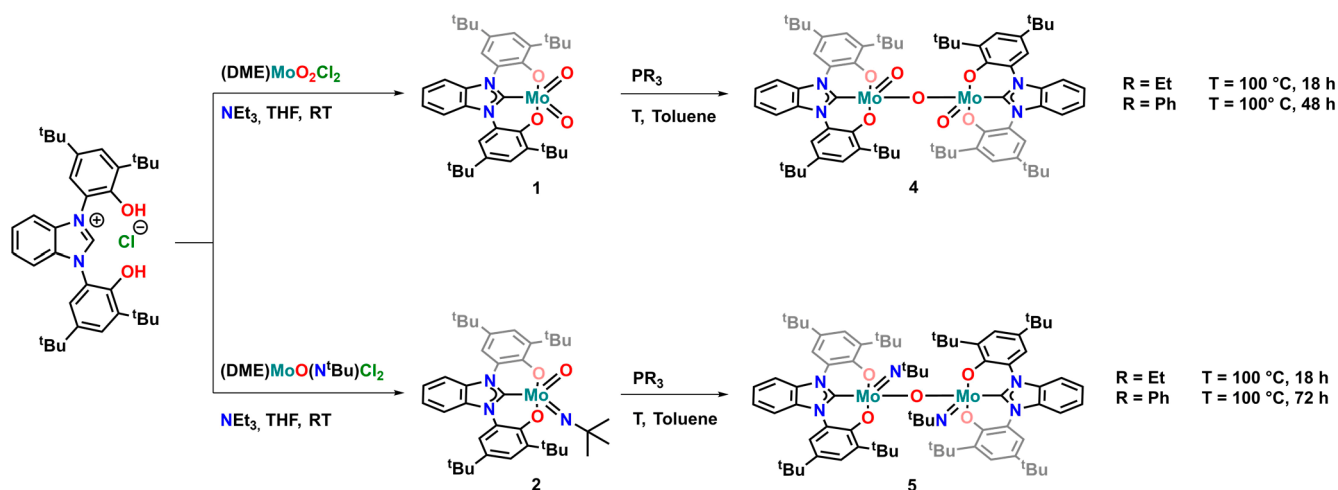
intermediate 6 (in case of 4). Both, 4 and 5 were found to exhibit a thermally accessible open-shell triplet state which is responsible for an unexpected paramagnetism in these complexes. Mechanistic details of the catalytic deoxygenation of nitroarenes will be discussed, shedding light on the fate of the catalyst and potential routes how nitroarene reduction is facilitated.

RESULTS AND DISCUSSION

As already mentioned, a crucial factor a (pre)catalyst must meet to be active in OATC, is to bind oxygen reversibly. Additionally, it has been shown in the past that deoxygenated metal complexes are prone to undergo (undesired) ligand decompositions.⁸³ To ensure that our NHC complexes 1 and 2 meet both requirements, we initially examined their OAT reactivity using phosphines as oxygen atom acceptors. Using both triethyl- or triphenylphosphine ($\text{P}(\text{Et})_3$ or $\text{P}(\text{Ph})_3$) resulted in the clean formation of two new complexes 4 and 5 at 100 °C (Scheme 2). Complex 4 could be isolated as a reddish brown (Figure S29), and complex 5 could be isolated as a dark green (Figure S30) powder in moderate yields of 56–81%. In contrast, using trimethylphosphine ($\text{P}(\text{Me})_3$) at various temperatures (room temperature to 100 °C) only resulted in the isolation of complicated mixtures which could not be further separated. Upon further characterization of 4 and 5, we found both complexes to display unexpected (paramagnetic) NMR characteristics (Figure 2).

Both NMRs show paramagnetically shifted peaks ranging from 10.3 to 1.30 ppm for complex 4 and from 8.50 to –1.11 ppm for complex 5. The presence of twelve distinct resonances (Figure 2) furthermore indicates the formation of an asymmetric (dinuclear) complex in solution. This is unexpected, since previous deoxygenations of molybdenum(VI) dioxo complexes resulted in the formation of either mononuclear $\text{Mo}(\text{IV})$ or symmetric dinuclear μ -oxo $\text{Mo}(\text{V})$ complexes.³⁵ The latter are formed if the steric bulk of the ligands is too small, allowing putative molybdenum(IV) complexes to comproportionate with the remaining molybdenum(VI) complexes to form μ -oxo bridged dinuclear molybdenum(V) complexes.³⁰ While solid-state structures (*vide infra*) suggested the presence of a C_{2v} symmetric species, only C_s symmetry is observed in solution. To test if large

Scheme 2. Deoxygenation of Complex 1 or 2 to Corresponding Oxo-Bridged Dimers 4 and 5 Using Either Triethyl- Or Triphenylphosphine



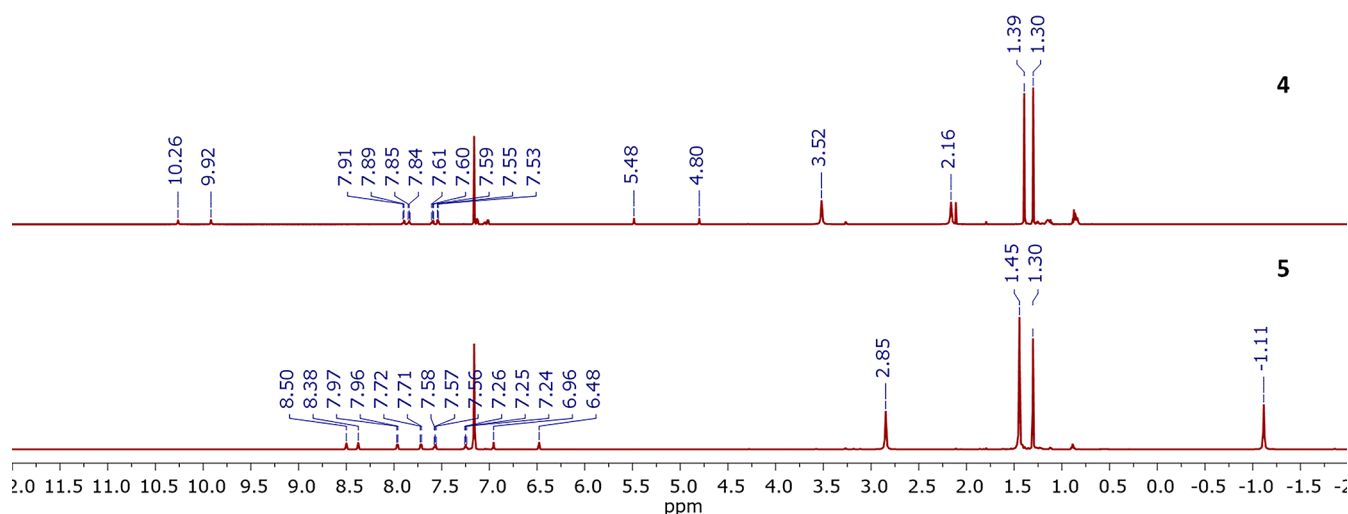


Figure 2. Proton NMR signatures of the new dimeric oxo bridged complexes **4** and **5** showing unexpected paramagnetically shifted resonances.

rotational barriers, e.g., along the μ -oxo unit, could be responsible for lowering the symmetry in solution, we performed variable-temperature (VT) NMR in the range of 243–333 K (instrumentation limits). Although we have seen an approach between the resonances in this temperature range, coalescence of the signals could not be reached (Figures S2 and S9).

Due to the paramagnetic nature of complexes **4** and **5**, clear assignments of the NMR signals cannot be made. However, for complex **5** we have been able to observe resonances at δ 392.3 and 391.5 ppm in the $^{13}\text{C}\{^1\text{H}\}$ spectrum most likely corresponding to the benzimidazolylidene carbene atoms. Additionally, for complex **5** we have been able to observe the ^{15}N chemical shift using ^1H – ^{15}N -HMBC NMR spectroscopy, showing a signal at δ 502.7 ppm corresponding to the *N*-*tert*-butyl imido ligand. The presence of two distinct carbene resonances in **5** further supports the presumption of an asymmetric dinuclear species in solution; the abnormal chemical shifts supports the paramagnetic nature of the complexes. To unambiguously prove the paramagnetic nature of the complexes, we measured its magnetic moment using the Evans method in solution. This revealed an effective magnetic moment of $2.22 \mu_{\text{B}}$ ($1.11 \mu_{\text{B}}$ per Mo) and $1.96 \mu_{\text{B}}$ ($0.98 \mu_{\text{B}}$ per Mo-ion) μ_{B} for **4** and **5** respectively. These values are substantially lower than the spin only values of $1.73 \mu_{\text{B}}$ expected for an isolated d^1 configured Mo(V) ion,⁸⁴ which would be anticipated if no antiferromagnetic coupling between the molybdenum centers existed. 2D-NMR techniques (COSY, HSQC, and HMBC, Figures S4–S6 for **4** and Figures S11–S13 for **5**) as well as ^1H DOSY NMR (Figures S7 and S15) furthermore unambiguously proved the presence of a single (asymmetric) complex in solution. It is noteworthy at this point that in the case of complex **4** ^1H - and ^{31}P -NMR spectra show the presence of uncoordinated triethylphosphine oxide (δ ^{31}P = 46.2 ppm), which we have not been able to remove despite copious hexane washing or recrystallization.

X-ray quality crystals of both complexes were grown by slow diffusion of pentane (for **4**) or hexane (for **5**) into a concentrated benzene solution of the complexes at room temperature. To our delight, the structural investigation, together with the results from NMR spectroscopy (*vide supra*) unambiguously proved that our NHC ligand is inert toward metal deoxygenations. Unfortunately, for complex **5**,

we have only been able to obtain low-quality crystals, and the pronounced air sensitivity of **5** (<1 min in the crystalline form) prevented us from obtaining high-quality data, prohibiting a reliable discussion of any bond parameters in **5**. Nevertheless, the connectivity in **5** could be unambiguously determined, and from the similarity of the NMR characteristics of complexes **4** and **5**, it can be assumed that the structural parameters follow the same tendencies. Both complexes crystallize in the monoclinic system in the space groups $P2_1/n$ (for **4**) and $C2/c$ (for **5**) with various strongly disordered solvent molecules (benzene and hexane) in the lattice, which needed to be removed by SQUEEZE techniques (see the Supporting Information for further details). For complex **4**, we have also been able to detect 0.5 equivalents of non-coordinated triethylphosphine in the asymmetric unit. Both complexes **4** and **5** form μ -oxo bridged dimers in solution resulting in a 5-fold coordination of each molybdenum center creating a slightly distorted square pyramidal (τ_5 = 0.10 for Mo1 and τ_5 = 0.03 for Mo1A for complex **4**, Figure 3) environment around the molybdenum ions. The molybdenum carbene distances Mo1–C1 and Mo1–C1A in complex **4** were found to be 2.181(4) and 2.182(4) Å and are slightly shorter compare to **1** (2.193(4) Å).⁶⁸ The oxo bridge in complex **4** was found to be symmetric, displaying Mo–O distances of 1.903(3) and 1.892(3) Å for Mo1–O10 and Mo1A–O10, respectively, with a Mo–O–Mo angle of 154.6(2)°. Further details on the crystallographic structure and structural parameters can be found in Tables S1 and S2.

In summary, the structural data indicate a molybdenum(V)–molybdenum(V) configuration of the complex. However, in the past, μ -oxo bridged molybdenum(V)–molybdenum(V) complexes have been found to be diamagnetic, exhibiting strong antiferromagnetic coupling between the two molybdenum centers.^{85–90} This is in stark contrast to the paramagnetic NMR signatures and the obtained magnetic moments in solution of our systems. To get further insight into the electronic structure of the complex, computational investigations were carried out at both the DFT (B3PW91) and CASSCF level (see Figure 4; for further details, see the Supporting Information, section 8). The geometries of complexes **4** and **5** were optimized at the DFT level for different spin states (singlet, triplet, and quintet). For complex **4**, the geometry agrees with the experimental one (see Table

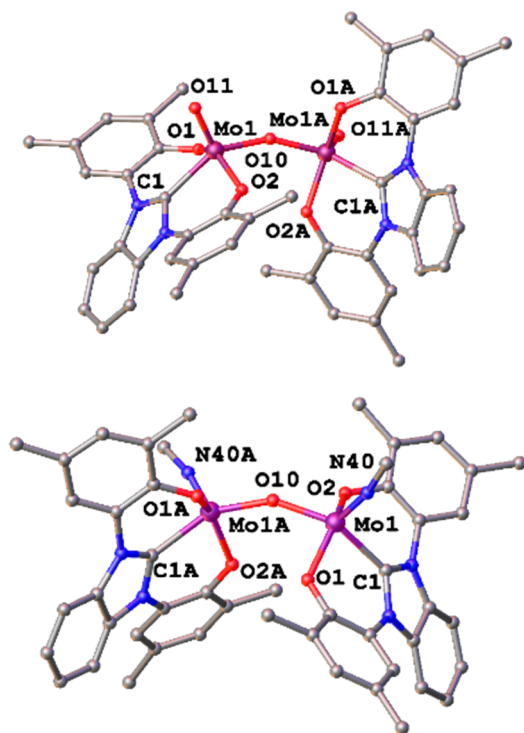


Figure 3. Molecular structures of complex 4 (top) and 5 (bottom). Hydrogen atoms, *tert*-butyl groups and lattice solvents have been omitted for clarity.

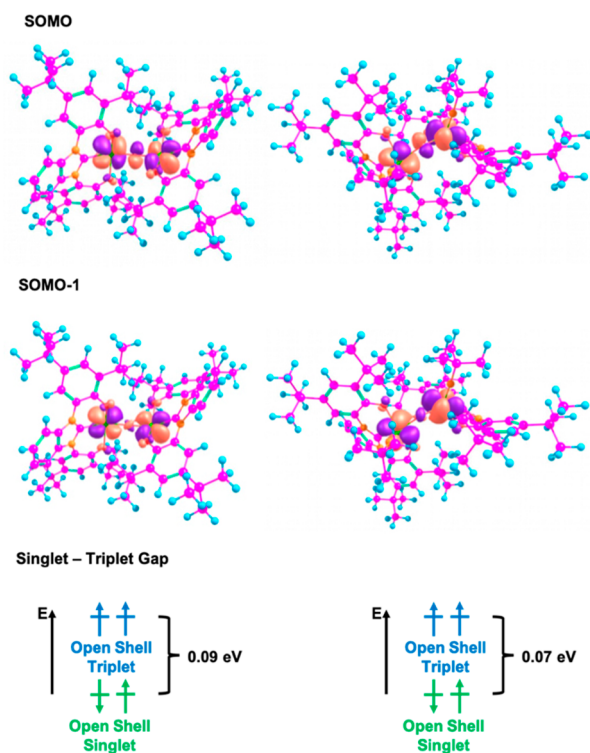


Figure 4. Frontier orbitals of complex 4 (left) and 5 (right) and the corresponding energy differences between the open-shell singlet ground state and the open-shell triplet excited state of complex 4 and 5 calculated by CASSCF.

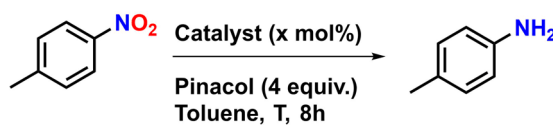
S2) and appears to be not much influenced by the spin state. Among others, the Mo1–C1 distance is very well reproduced (2.18 Å) as is the Mo1–O10 distance (1.88 Å). The Mo1–O–

Mo1A angle is a little bit too open (167° vs 154°). Although it was not possible to obtain high-quality X-ray data for complex 5, the computational structure was compared with that of complex 4. The bridging Mo1–O10 distance is slightly longer in 5 than that in 4 (1.90 Å vs 1.88 Å) but within the same range. Similarly, the Mo–C1 distance is essentially the same (2.17 Å in 5 vs 2.18 Å in 4) and the Mo1–O–Mo1A angle is found to be around 153° (see Table S2 for further detail). The electronic structures of the two complexes were then investigated using CASSCF calculations. CAS(6,5) calculations were then conducted for the two complexes in order to check the nature of the ground state and of the excited states. In both cases, the ground state is found to be an open-shell singlet formed from two Mo(V) d¹ centers. This open-shell singlet is therefore responsible for a TIP behavior at low temperature, that would account for the low magnetic moment found for the two complexes, as demonstrated by Booth.^{91–95} Moreover, the first excited state is in both cases, the associated triplet and is very close in energy (0.09 eV for complex 4 and 0.07 eV for complex 5). Thus, the triplet state can be populated at room temperature which increases the magnetic moment of the two complexes. The other excited states, accounting for lower oxidation state of Mo, are at least 2.1 eV higher in energy. Thus, the computational investigations of complexes 4 and 5 are clearly indicating the presence of two molybdenum(V) ions that are antiferromagnetically coupled in an open-shell singlet ground state but with the open-shell triplet state being thermally accessible, leading to the magnetic moments observed by Evans method (*vide supra*).

Catalytic Deoxygenations. Knowing that complexes 1 and 2 can be deoxygenated and that the NHC ligand is not affected under these conditions, we next investigated the catalytic potential of these complexes in the deoxygenation of nitroarenes. As an initial starting point, we have tried to deoxygenate *p*-nitrotoluene using 1 mol % catalyst (1 or 2) and triphenylphosphine as a sacrificial oxygen atom acceptor at 130 °C. Unfortunately, these conditions were found to be very inefficient, resulting in no conversion at all. However, taking a deeper look into the stoichiometry of this reaction, this is not surprising as the efficient conversion of nitroarenes to anilines requires the presence of at least two protons. Switching from triphenylphosphine to pinacol as a green and environmentally benign reducing agent,⁹⁶ we found the clean and fast conversion of *p*-nitrotoluene to toluidine within 8 h using only 1 mol % loading of the corresponding catalysts at 130 °C (Figure S33). Lower temperatures, e.g., 110 °C, or omitting the catalysts were both found to be detrimental to the catalytic reaction (Table 1). Inspired by the relatively low catalyst loading of only 1 mol %, we were further interested how much the catalyst loading could be decreased.

Indeed, using only 0.25 mol % resulted in similar results, and we found full conversion of *p*-nitrotoluene after 8 h of reaction time (Table 1 and Figure S33). To set this into relation, we also calculated the corresponding TON and TOF values. At 0.25 mol % loading, the highest TOF we observed corresponds to about 50 turnovers per hour. This is a roughly 5-fold increase compared to previous reports by Sanz and co-workers.⁹⁶ Comparison of the reaction time profiles performed on the reaction with 0.25 mol % of catalyst using either complex 1 or 2 as a precatalyst shows a very similar progression of the reaction (Figure S33), further indicating that the active species forming might be identical for both of these complexes.

Table 1. Condition Screening for the Deoxygenation of *p*-Nitrotoluene Using Complexes 1 or 2 as (Pre-)Catalysts^a



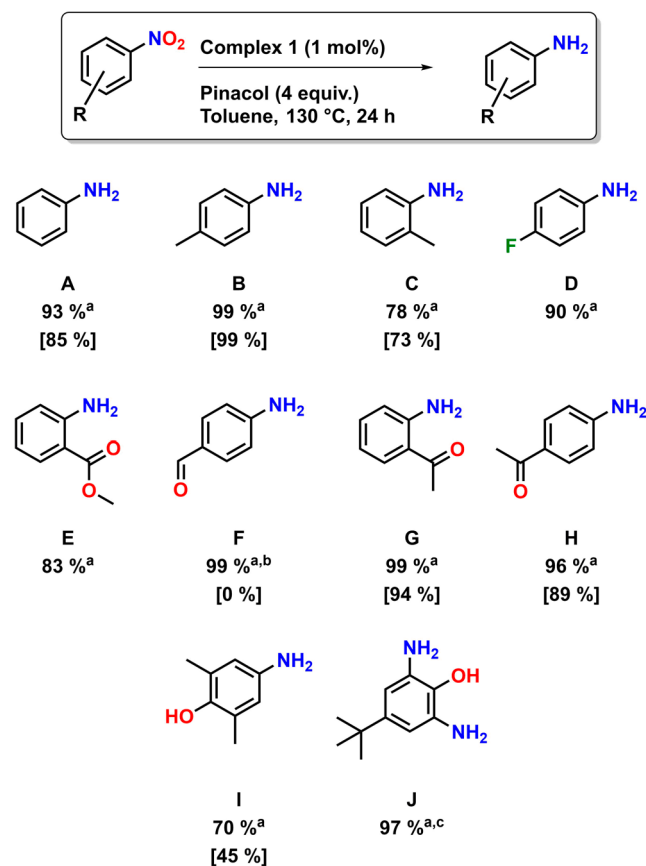
| cat. | mol % | T (°C) | conv. | TON | TOF (h ⁻¹) |
|--|-------|--------|-------|------|------------------------|
| 1 | 1 | 130 | 99% | 100 | 12.5 |
| 2 | 1 | 130 | 99% | 100 | 12.5 |
| 1 | 1 | 110 | 0% | 0 | 0 |
| 2 | 1 | 110 | 0% | 0 | 0 |
| 1 | 0.5 | 130 | 99% | 200 | 25 |
| 2 | 0.5 | 130 | 99% | 200 | 25 |
| 1 | 0.25 | 130 | 99% | 400 | 50 |
| 2 | 0.25 | 130 | 99% | 400 | 50 |
| MoO ₂ Cl ₂ (DMF) ₂ ^b | 5 | 130 | 93% | 18.6 | 9 |

^aConversions are determined via GC using mesitylene as an internal standard. ^bReaction has been carried out for 2 h in xylene; see ref 96.

Since water is liberated during the reaction (*vide supra*), hydrolysis of the imido group in complex 2 to form complex 1 is very likely to happen. Due to these circumstances and because the synthesis of complex 1 is more convenient compared to 2,⁶⁸ we decided to focus on complex 1 for further studies, regarding the mechanism and the substrate scope of the catalytic reaction.

Elucidating the substrate scope of the catalytic deoxygenation reaction, we decided to raise the catalyst loading to 1 mol %, to make sure challenging nitroarenes can also be efficiently converted to the corresponding anilines. The catalytic reactions have been carried out using four equivalents of pinacol per nitro group at 130 °C for 24 h. The results have been summarized in Scheme 3. We found that complex 1 efficiently catalyzes the deoxygenation of unfunctionalized, alkyl substituted nitroarenes, including *o*-nitrotoluene as well as unsubstituted nitrobenzene. This gave access to the corresponding anilines in good yields, after a short workup (see the Supporting Information). Turning our focus on the functional group tolerance, we initially examined *o*- and *p*-nitroacetophenone, which could both be efficiently converted into the corresponding anilines in isolated yields of 94% (ortho) and 89% (para). In contrast, using *p*-nitrobenzaldehyde and despite the full consumption of *p*-nitrobenzaldehyde, we have not been able to isolate any *p*-aminobenzaldehyde from the reaction. The crude reaction mixture indicated the formation of a complex mixture of products, displaying various imine signals in the low-field region of its ¹H NMR. We assume that due to the high temperature necessary for the reaction to proceed, the aldehyde condensates directly with the formed amine to (polymeric) imines. Polymerization of amino-benzaldehydes has also been seen previously in the literature.⁹⁷ Turning to more electron-withdrawing substituents such as fluorides and esters, we have also observed moderate to good conversions of the corresponding nitroarenes. However, this indicates that for strongly electron-withdrawing substituents the higher catalyst loadings might be necessary to reach full conversion of the substrates. Switching to electron-donating substituents, we found 70% conversion of 2,6-dimethyl-4-nitrophenol, which could be isolated in a yield of 45% after workup from the reaction mixture. Probing the efficiency of our catalyst in the reduction of multiple nitro groups at once,

Scheme 3. Scope of the Catalytic Deoxygenation Reactions Using Complex 1 as a Precatalyst

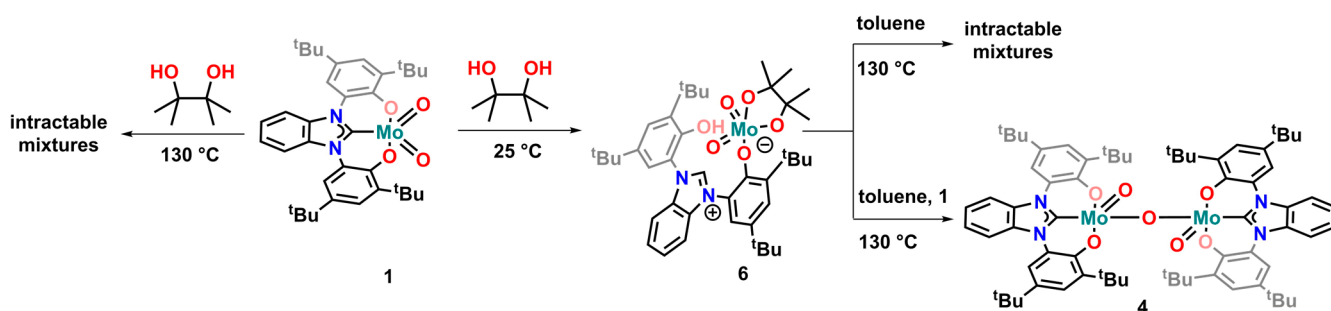


^aYields of the corresponding nitroarenes determined by GC measurements using mesitylene as an internal standard. ^bConversion of 4-nitrobenzaldehyde. No formation of the corresponding aniline could be detected by GC. ^cA total of 8 equiv of pinacol have been applied. Values in brackets are isolated yields.

we also investigated the reduction of 4-(*tert*-butyl)-2,6-dinitrophenol with 8 equiv of pinacol (4 equiv per nitro group) which resulted in the full conversion of nitroarene. The latter two examples show that protic phenols (and potentially other substrates up to $pK_a = 7$) can be efficiently deoxygenated under the conditions present. In summary, our substrate screening shows that even at catalyst loadings of only 1 mol % complex 1 is an efficient (pre)-catalyst for the deoxygenation of various nitroarenes with excellent group tolerance.

Mechanistic Investigations. Having established our molybdenum complexes 1 and 2 to be indeed very active (pre)catalyst for the deoxygenation of nitroarenes, we next turned our interest toward how the reactions proceeds mechanistically. Since the time-reaction profiles recorded (Figure S33) indicate that the active species formed could be the same for both (pre)catalysts 1 and 2, the following investigations will be limited to complexes 1 and 4. Special emphasis was put on the question of whether isolated μ -oxo complex 4 could be a potential intermediate in the catalytic cycle. Therefore, two major question needed to be addressed: (a) Is the oxo-bridged complex 4 also formed if pinacol is used as the sacrificial reductant? (b) Is the μ -oxo-bridged complex 4 capable of deoxygenating nitroarenes and other possible intermediates, e.g., nitrosoarenes, formed during the deoxygenation processes?

Scheme 4. Test Reaction under Various Conditions to Prove the Formation of Complex 4 Using Pinacol as the Sacrificial Reductant



In analogy to Sanz and co-workers, who were able to isolate μ -oxo-bridged complexes $\text{MoO}_3\text{Cl}_4(\text{DMF})_4$ ⁹⁶ from the reaction between $\text{MoO}_2\text{Cl}_2(\text{DMF})_2$ and pinacol, we also heated complex 1 in the presence of excess pinacol at 130 °C overnight. However, instead of forming complex 4, this only resulted in the formation of intractable mixtures. Switching to less harsh conditions, the reaction between equimolar amounts of pinacol and complex 1 at room temperature affords a new complex, 6, which can be isolated in good yields of 96% (Method A, see SI) as a white solid. The ^1H NMR spectrum of complex 6 showed C_1 symmetry in solution and the presence of four singlets between 1.11 and 0.5 ppm integrating to 3:3:3:3 protons clearly indicate the presence of coordinated pinacol. Surprisingly, the ^{13}C NMR showed no resonance above 155.4 ppm, which suggests the absence of an NHC ligand. Aside from the structural proof (*vide infra*), the assignment of the proposed structure of complex 6 in Scheme 4 can be confidently made based on several features in the 2D-NMR data of the isolated material. Protonation of the benzimidazolium unit can be unambiguously assigned by the presence of a cross peak at 8.87/143.5 ppm in the ^1H - ^{13}C HSQC NMR (see Figure S19).⁸¹ Protonation of a phenolate unit is furthermore indicated by the presence of three features: First, no coupling of the proton resonating at 8.25 ppm to any other arene proton is observed neither in the 1D- ^1H NMR nor in ^1H - ^1H -COSY NMR. Second, the proton was found to couple to a quaternary arene carbon atom in the ^1H - ^{13}C HMBC at 8.25/141.8 ppm, which was also found to couple to one *tert*-butyl group at 1.51/141.8 ppm (Figure S20). Third, while the carbon atom at 155.4 ppm corresponding the deprotonated two C=O group was found to couple to only two arene protons (7.57/155.4 and 7.32/155.4 ppm), the carbon atom of the protonated C=O group resonates at 149.7 ppm showing couplings to two arene protons (7.61/149.7 and 7.09/149.7 ppm) and the additional OH-proton at 8.25/149.7 ppm. This coupling pattern can only be observed if one of the phenolate residues is protonated. Protonation of the benzimidazolylidene unit as well as the phenolate unit would last explain the obtained C_1 symmetry in solution. Ultimate proof for the protonation of the benzimidazolylidene moiety in 6 was obtained by X-ray diffraction analysis. X-ray quality crystals of 6 were obtained after two days from a solution of 1 in benzene layered by a solution of pinacol in benzene at room temperature. The complex crystallizes in the monoclinic space group $C2/c$ with two molecules of benzene in the asymmetric unit. The molybdenum center in 6 is five-coordinate by only oxygen donors in a strongly distorted square pyramidal fashion ($\tau_5 = 0.45$). The Mo1–C1 distance was found to be 3.684(3) Å clearly showing no interaction between the metal center and

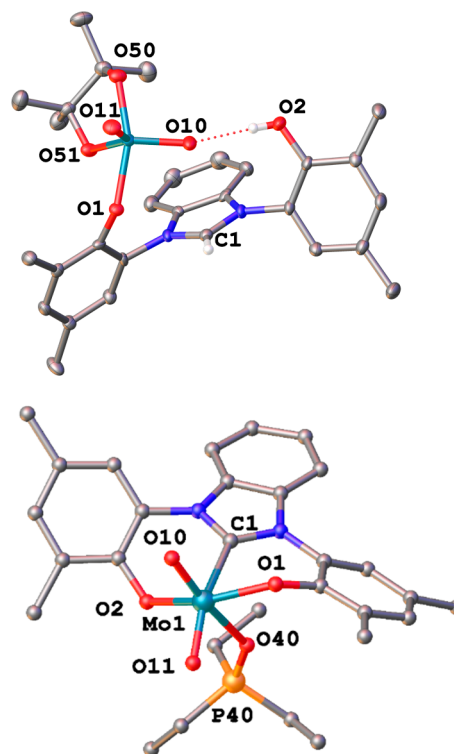
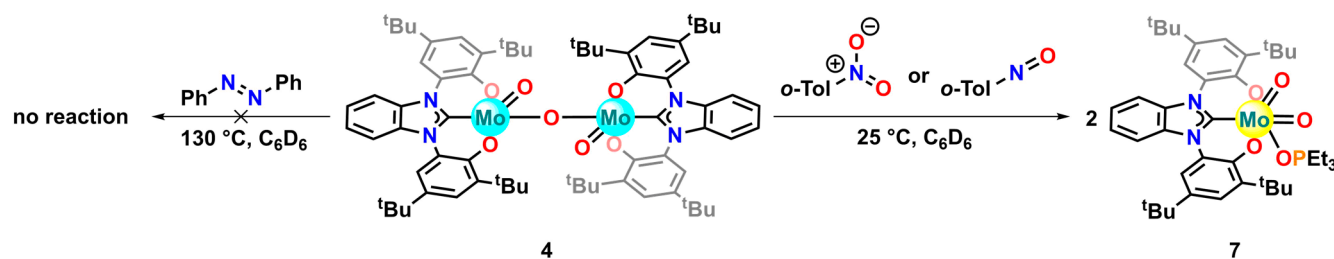


Figure 5. Molecular structures of complexes 6 (top) and 7 (bottom). Hydrogen atoms, *tert*-butyl groups, and additional lattice solvents have been removed for clarity.

the former carbene center. Additionally, the benzimidazolium-2H proton can be found in the Fourier map, unambiguously confirming the protonation of the benzimidazolylidene unit. Notably, the protonated phenol group of the ligand displays strong hydrogen bonding to one of the Mo=O oxo ligands (compare Figure 5, top structure). Interestingly, the protonation of the NHC unit is in strong contrast to our and Buchmeiser's previous findings demonstrating the Mo–NHC bond stable toward protic reagents and water.^{67,68} However, it might be worth mentioning that in Buchmeiser's case, the inherent stability of the cationic Mo–NHC complexes toward protic substrates can be partly explained by the delocalization of the positive charge across the NHC ligand, rendering it to be less basic. Additionally, the MoO₂ fragment is more Lewis acidic compared to the imido-alkylidene fragment, which facilitates protonation of the NHC moiety in such complexes. This is in line with seminal reports by Herrmann and co-workers, stating that the NHC ligand in dioxo-molybdenum NHC complexes can be easily hydrolyzed.⁵⁵ Thus, these

Scheme 5. Stoichiometric Reactions between Complex 4 and *o*-Nitro/Nitrosotoluene and Azobenzene to Investigate the Mechanism of the Catalytic Deoxygenation Reaction of Nitrotoluene^a



^aColor coding: Mo^{VI}: yellow, Mo^V: turquoise. Note that the triethylphosphine oxide ligand in 7 results from an unremovable impurity of triethylphosphine oxide in complex 4.

findings suggest that the stability of the NHC-Mo bond cannot be generally determined and is depending on various effects like the substitution pattern on the Mo(VI) fragment and the coordination mode, e.g., potential chelators such as pinacol, of the protic substrate used.

To seek further evidence if complex 4 can be formed from complex 6, we heated 6 to 130 °C which resulted in catastrophic decompositions (Figure S35). Acknowledging the fact that 4 most likely forms via the synproportionation of a Mo(IV) and a Mo(VI) complex, we repeated the experiment in the presence of 1 equiv of complex 1. Notably, these conditions led to the formation of desired compound 4 (see Figure S36). However, we want to emphasize that the reaction under these conditions is far from clean, and given the fact that the carbene unit can be protonated under catalytic conditions, the formation of other molybdenum complexes without NHC coordination, which could be potential catalysts for the deoxygenation reaction, cannot be fully excluded (*vide infra*).⁹⁶

Stoichiometric Deoxygenation Reactions. Having shown that the formation of μ -oxo complex 4 is indeed possible under catalytic conditions, our next focus was to explore if 4 would be a potentially active species in the deoxygenation of nitroarenes. Notably, Sanz and co-workers stated earlier that MoO₃Cl₄(DMF)₄ has similar catalytic properties as the parent MoO₂Cl₂(DMF)₂ when pinacol is used as a sacrificial reductant.⁹⁶ To our delight, mixing stoichiometric amounts of 4 with *o*-nitrotoluene resulted in the complete consumption of complex 4 after 96 h at room temperature (see Figure S38). However, NMR spectroscopy revealed that not the expected complex 1 is reformed under these conditions, but a new complex 7 is formed. (Scheme 5). Remembering that complex 4 could only be obtained with uncoordinated triethylphosphine oxide as an impurity, we have been able to identify this new complex to be triethylphosphine oxide adduct 7 by ¹H and ³¹P NMR spectroscopy. It is noteworthy that complex 7 can also be obtained independently by the reaction of 1 with 1 equiv of triethylphosphine oxide.⁹⁸ The presence of a resonance at $\delta = 194.5$ ppm in the ¹³C{¹H} NMR spectrum unambiguously confirms the assignment of a NHC complex. The phosphorus signal shifts from 46.2 to 55.7 ppm, supporting the coordination of triethylphosphine oxide. X-ray quality crystals of 7 could be obtained by storing a very concentrate solution of 7 in toluene at -40 °C for 3 days (Figure 5). Since the structural metrics resemble the ones found in complex 1,⁶⁸ we would like to resign on a detailed discussion here. Additional information regarding the bond angles and crystal metrics can be found in Table S1 and S2. We would like to note at this point that the deoxygenation of *o*-

nitrotoluene using complex 5 is completed within a few seconds, and mechanistic investigations using an internal standard proves that 2 equiv of anticipated complex 2 are reformed under these conditions (Figure S37 and Figure S41).

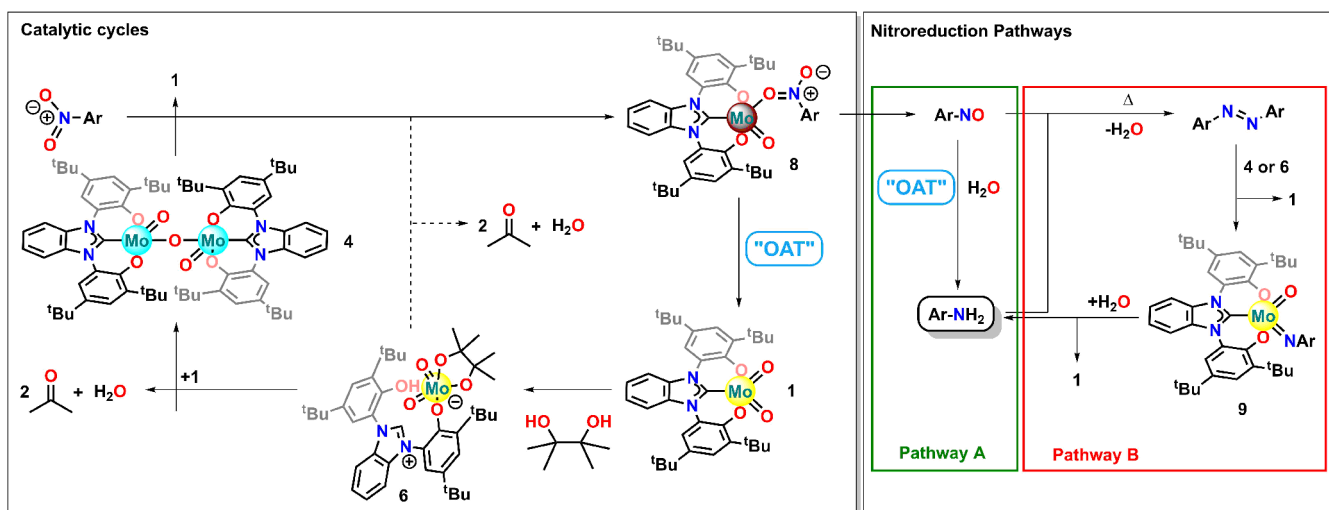
The fact that complex 4 is indeed capable of efficiently deoxygenating *o*-nitrotoluene suggests it to be a potential intermediate in the catalytic deoxygenation of nitroarenes. Since Arnold and co-workers have recently shown that metal complexes with multiconfigurational ground states can exhibit unique and unexpected reactivity patterns,^{99–101} we were curious if the spin state (singlet vs triplet) of our complexes would also have an influence on the activation barrier of the deoxygenation reaction. Therefore, we calculated the energy profile of the deoxygenation reaction of nitrobenzene mediated by complex 4 in dependency of the spin state (Figure S45). This revealed the coordination of nitrobenzene to be exothermic, leading to a splitting of 4 to make complex 1 and the molybdenum(IV) complex 8 (see also Scheme 6). Processing along the reaction coordinate revealed that effective barrier for the deoxygenation process is lower by 5 kcal/mol if a triplet state of the catalyst is assumed compared to the singlet state. This strongly indicates that the spin state of the catalyst has a major impact on the catalytic potential of these metal complexes, which might be another explanation for the high catalytic potential of the complexes (*vide supra*).

Despite showing that complexes 4 and 5 could be both catalytically active species in the deoxygenation of nitroarenes, we were further interested in the role of complex 6 during the catalytic reaction. Although we have shown that 4 can be made under catalytic conditions by heating an equimolar mixture of complexes 1 and 6 (*vide supra*), the large excess of pinacol (compared to precatalyst 1) used in the reaction suggests that complex 6 might also play an important role in the catalytic reaction. Despite we have not been able to isolate any species from the thermal decomposition of complex 6 at 130 °C (Figure S35), adding an equimolar amount of 4-nitrotoluene prior to heating facilitated the clean reformation of complex 1 at 130 °C after 18 h, along with the consumption of the nitroarene and the liberation of 2 equiv of acetone (resulting from the reductive splitting of the pinacol bound to the Mo center in 6, compare Figure S43). This clearly states that not only complex 4 could be a potential active species but also 6 might also play a vibrant role during the catalytic cycle.

Pathways of Nitroarene Deoxygenation Catalysis.

Looking deeper into how the reduction of nitroarenes could be facilitated mechanistically, there are two different potential routes that can occur (Scheme 6). Pathway A would cover the reduction of nitroarenes via nitrosoarenes and its direct

Scheme 6. Possible Catalytic Pathways and Intermediates of the Deoxygenation of Nitroarenes to Anilines Mediated by Complex 1 via either 4 or 6 as a potentially active species.^a



^aColor coding: Mo^{VI}: yellow, Mo^V: turquoise, Mo^{IV}: brown.

conversion to the corresponding aniline. However, since the catalytic reaction is carried out at 130 °C, it is also possible that once small amounts of anilines have formed these could condensate with nitrosoarenes present to form azoarenes. The latter could then be activated by complex 4 or 6, and hydrolysis of the corresponding imido complex 9 would lead to the desired aniline, reforming complex 1 (Pathway B, see Scheme 6).

Since complexes 4 and 5 were already shown to effectively deoxygenate *o*-nitrotoluene, we next examined its reactivity toward *o*-nitrosotoluene. Indeed, full conversion from 4 to 7 was achieved within 1 h at room temperature (Figure S39). To exclude that Pathway B, via the condensation to azobenzene, now plays an important role in the catalytic cycle, if 4 would be the active species in the catalytic cycle, we have investigated the stoichiometric reaction between 4 and azobenzene (Figure S40). Indeed, no reaction occurred even after 2 days at 130 °C, confirming complex 4 being incapable of splitting azobenzene.

In contrast, exploring the catalytic cycle and potentially intermediates with the pinacol complex 6, we found that 6 is besides deoxygenating nitroarenes (*vide supra* and Figure S43) also capable of splitting azobenzene stoichiometrically (Figure S44). Interestingly, we have not been able to isolate the anticipated oxo-imido complex 9 from the reaction mixture, but dioxo complex 1 was reisolated. Although this was unexpected in the first place, it can be rationalized by the fact that somewhere during the catalytic process water must be eliminated to reform the metal–carbene and metal–phenolate bonds. At 130 °C reaction temperature, water is very likely to hydrolyze any imido complex to reform the dioxo complex 1.¹⁰² The potential of 6 to split azobenzene is furthermore undermined by the fact that complex 1 reduces azobenzene to aniline catalytically using 4 equiv of pinacol as a reducing agent and a catalyst loading of 1 mol % within 4 h at 130 °C (Figure S34). Nevertheless, on re-examining the time conversion data (Figure S33), no azobenzene could be detected in the reaction mixtures. Although this is not clear proof that pathway A is the dominant path (it is possible that the reduction of azobenzene is extremely fast in solution, prohibiting the accumulation of a detectable concentration of it in solution), these results suggest

fairly well that the azobenzene route (pathway B) plays only a minor role for the catalytic reduction of nitroarenes to anilines mediated by NHC molybdenum complex 1. This can be further rationalized by the fact that *o*-nitrosotoluene is efficiently deoxygenated by complex 4 already at room temperature (*vide supra*), preventing the build up of higher nitrosoarene concentration and thus lowering the chances for the successful condensations of nitrosoarenes and anilines to form the corresponding azobenzenes under catalytic conditions (130 °C).

CONCLUSION

In conclusion, we have shown molybdenum(VI) complexes 1 and 2, reported earlier by our group,⁶⁸ are very active (pre)catalysts for the deoxygenation of nitroarenes to form anilines using pinacol as a green sacrificial reductant. Under the present conditions, we have been able to reduce the catalyst loading by up to a factor of 20, compared to previous reports⁴⁶ with an excellent tolerance of functional groups, except for *p*-nitro-benzaldehyde. For the latter, the high temperatures needed for the deoxygenation to proceed most likely induces the polymerization of the anticipated *p*-amino-benzaldehyde. Mechanistic investigations have shown that under catalytic conditions both, new dinuclear μ -oxo molybdenum(V) complexes 4 and 5 as well as the unexpected pinacolate complex 6 with a protonated benzimidazolium unit can be formed. Notably, 4 and 5 can also be formed by deoxygenation of parent complexes 1 and 2 with triethylphosphine as an oxygen atoms acceptor. Both complexes were found to adopt an unusual multiconfigurational configuration, with the open-shell-triplet state to be only marginally above the (expected) open-shell-singlet state in energy which allowed thermal population of the former state. This results in an unexpected paramagnetism for both complexes 4 and 5. Both complexes, 4 and 5, have been found to be excellent oxygen atoms acceptors at room temperature, efficiently deoxygenating nitroarenes and nitrosoarenes reforming parent complexes 1 and 2. Additionally, complex 6 deoxygenates nitroarenes at 130 °C (under catalytic conditions), also reforming complex 1. These results indicate that both the μ -oxo complexes as well as

benzimidazolium complex **6** could play an important role in the catalytic cycle. The activation barrier of the deoxygenation step was further shown to be dependent on the spin state of the complexes, and we found the barrier for complex **4** to be about 5 kcal/mol lower for the triplet state compared to that for the singlet state, which might further explain the excellent catalytic potential of complexes **1** and **2**. In addition, we shedded light on the mechanism of the reduction process, which most likely favors a stepwise, direct reduction from nitroarenes via nitrosoarenes to anilines. However, the results do not fully exclude the possibility of azoarenes as intermediates in the catalytic cycle as it has been observed for example in (transfer-)hydrogenations.¹⁵

Future work is necessary to determine the effect of the central carbene unit⁶⁹ on the activity of the molybdenum(VI) complexes in OAT reactions/catalysis, to lower the temperatures needed for effective OATC to proceed, to further elucidate and distinguish between the two possible active species. Additionally, we are aiming to indentify further modes of reactivity prompted by the unusual electronic structure of dinuclear complexes **4** and **5**.

■ ASSOCIATED CONTENT

SI Supporting Information

The Supporting Information is available free of charge at <https://pubs.acs.org/doi/10.1021/acs.organomet.0c00352>.

Compound structures (XYZ)

Synthetic details, NMR spectra, IR spectra, UV–vis spectra, GC traces, and crystallographic details for all compounds (PDF)

Accession Codes

CCDC 1993053, 1993054, and 2044177 contain the supplementary crystallographic data for this paper. These data can be obtained free of charge via www.ccdc.cam.ac.uk/data_request/cif, or by emailing data_request@ccdc.cam.ac.uk, or by contacting The Cambridge Crystallographic Data Centre, 12 Union Road, Cambridge CB2 1EZ, UK; fax: +44 1223 336033.

■ AUTHOR INFORMATION

Corresponding Authors

Laurent Maron – LPCNO, Université de Toulouse, INSA Toulouse, 31077 Toulouse, France; orcid.org/0000-0003-2653-8557; Email: laurent.maron@irsamc.ups-tlse.fr

Stephan Hohloch – University of Innsbruck, Faculty of Chemistry and Pharmacy, Institute of General, Inorganic and Theoretical Chemistry, 6020 Innsbruck, Austria; orcid.org/0000-0002-5353-0801; Email: Stephan.Hohloch@uibk.ac.at

Authors

Shenyu Liu – Paderborn University, Faculty of Science, Department of Chemistry, 33098 Paderborn, Germany

Jorge Ivan Amaro-Estrada – LPCNO, Université de Toulouse, INSA Toulouse, 31077 Toulouse, France

Marc Baltrun – Paderborn University, Faculty of Science, Department of Chemistry, 33098 Paderborn, Germany

Iskander Douair – LPCNO, Université de Toulouse, INSA Toulouse, 31077 Toulouse, France; orcid.org/0000-0002-7482-5510

Roland Schoch – Paderborn University, Faculty of Science, Department of Chemistry, 33098 Paderborn, Germany; orcid.org/0000-0003-2061-7289

Complete contact information is available at: <https://pubs.acs.org/doi/10.1021/acs.organomet.0c00352>

Author Contributions

The project was designed by S.H. Experimental work was conducted by S.L., M.B., and S.H. Theoretical investigations were performed by J.I.A.-E., I.D., and L.M. X-ray crystal analysis was performed by S.H. and R.S. The manuscript was written by S.L., S.H., and L.M. and proofread by all authors.

Notes

The authors declare no competing financial interest.

■ ACKNOWLEDGMENTS

We are grateful to the Daimler and Benz Foundation, to the Fonds der Chemischen Industrie, to the Young Academy of the North Rhine-Westphalian Academy of Sciences, Humanities and the Arts, to the Paderborn University and to the University of Innsbruck for funding of this work. Prof. Dr. Jan Paradies is kindly acknowledged for helpful discussion. The authors thank Philipp Boos for synthesis of ligand precursor [H₃L]Cl. Our special thanks go to Dr. Hans Egold from Paderborn University and to Prof. Dr. Christoph Kreutz from the University of Innsbruck for assistance with NMR measurements. Finally, S.H. expresses his special thanks to Prof. Dr. Wolfgang Kaim whose lectures, passion for unexpected electronic structures of metal complexes, and continuous support have been one of the foundation stones for pursuing a career in academia. This work is dedicated to Prof. Dr. Wolfgang Kaim on the occasion of his 70th birthday.

■ REFERENCES

- (1) Rogers, K. A.; Zheng, Y. Selective Deoxygenation of Biomass-Derived Bio-oils within Hydrogen-Moderate Environments: A Review and New Insights. *ChemSusChem* **2016**, 9 (14), 1750–1772.
- (2) Shiramizu, M.; Toste, F. D. Deoxygenation of biomass-derived feedstocks: oxorhenium-catalyzed deoxydehydration of sugars and sugar alcohols. *Angew. Chem., Int. Ed.* **2012**, 51 (32), 8082–8086.
- (3) Kim, S.; Kwon, E. E.; Kim, Y. T.; Jung, S.; Kim, H. J.; Huber, G. W.; Lee, J. Recent advances in hydrodeoxygenation of biomass-derived oxygenates over heterogeneous catalysts. *Green Chem.* **2019**, 21 (14), 3715–3743.
- (4) Yi, J.; Liu, S.; Abu-Omar, M. M. Rhenium-catalyzed transfer hydrogenation and deoxygenation of biomass-derived polyols to small and useful organics. *ChemSusChem* **2012**, 5 (8), 1401–1404.
- (5) Rubio-Presa, R.; Fernández-Rodríguez, M. A.; Pedrosa, M. R.; Arnáiz, F. J.; Sanz, R. Molybdenum-Catalyzed Deoxygenation of Heteroaromatic N-Oxides and Hydroxides using Pinacol as Reducing Agent. *Adv. Synth. Catal.* **2017**, 359 (10), 1752–1757.
- (6) Jagadeesh, R. V.; Surkus, A.-E.; Junge, H.; Pohl, M.-M.; Radnik, J.; Rabeah, J.; Huan, H.; Schünemann, V.; Brückner, A.; Beller, M. Nanoscale Fe₂O₃-based catalysts for selective hydrogenation of nitroarenes to anilines. *Science* **2013**, 342 (6162), 1073–1076.
- (7) Balaraman, E.; Gnanaprakasam, B.; Shimon, L. J. W.; Milstein, D. Direct hydrogenation of amides to alcohols and amines under mild conditions. *J. Am. Chem. Soc.* **2010**, 132 (47), 16756–16758.
- (8) Wienhöfer, G.; Baseda-Krüger, M.; Ziebart, C.; Westerhaus, F. A.; Baumann, W.; Jackstell, R.; Junge, K.; Beller, M. Hydrogenation of nitroarenes using defined iron-phosphine catalysts. *Chem. Commun.* **2013**, 49 (80), 9089–9091.
- (9) Wienhöfer, G.; Sorribes, I.; Boddien, A.; Westerhaus, F.; Junge, K.; Junge, H.; Llusar, R.; Beller, M. General and selective iron-

catalyzed transfer hydrogenation of nitroarenes without base. *J. Am. Chem. Soc.* **2011**, 133 (32), 12875–12879.

(10) Wang, D.; Astruc, D. The golden age of transfer hydrogenation. *Chem. Rev.* **2015**, 115 (13), 6621–6686.

(11) Hopmann, K. H.; Bayer, A. Enantioselective imine hydrogenation with iridium-catalysts: Reactions, mechanisms and stereo-control. *Coord. Chem. Rev.* **2014**, 268, 59–82.

(12) Ikariya, T.; Blacker, A. J. Asymmetric transfer hydrogenation of ketones with bifunctional transition metal-based molecular catalysts. *Acc. Chem. Res.* **2007**, 40 (12), 1300–1308.

(13) Malacea, R.; Poli, R.; Manoury, E. Asymmetric hydrosilylation, transfer hydrogenation and hydrogenation of ketones catalyzed by iridium complexes. *Coord. Chem. Rev.* **2010**, 254 (5–6), 729–752.

(14) Ramollo, G. K.; Strydom, I.; Fernandes, M. A.; Lemmerer, A.; Ojwach, S. O.; van Wyk, J. L.; Bezuidenhout, D. I. Fischer Carbene Complexes of Iridium(I) for Application in Catalytic Transfer Hydrogenation. *Inorg. Chem.* **2020**, 59 (7), 4810–4815.

(15) Hohloch, S.; Suntrup, L.; Sarkar, B. Arene–Ruthenium(II) and – Iridium(III) Complexes with “Click”-Based Pyridyl-triazoles, Bis-triazoles, and Chelating Abnormal Carbenes: Applications in Catalytic Transfer Hydrogenation of Nitrobenzene. *Organometallics* **2013**, 32 (24), 7376–7385.

(16) Bolje, A.; Hohloch, S.; Košmrlj, J.; Sarkar, B. RuII, IrIII and OsII mesoionic carbene complexes: efficient catalysts for transfer hydrogenation of selected functionalities. *Dalton Trans.* **2016**, 45 (40), 15983–15993.

(17) Brandts, J. A. M.; Berben, P. H. Application of Immobilized Rhodium Catalyst Precursors in Enantio- and Chemoselective Hydrogenation Reactions. *Org. Process Res. Dev.* **2003**, 7 (3), 393–398.

(18) Gorgas, N.; Ilic, A.; Kirchner, K. Chemoselective transfer hydrogenation of aldehydes in aqueous media catalyzed by a well-defined iron(II) hydride complex. *Monatsh. Chem.* **2019**, 150 (1), 121–126.

(19) Himeda, Y.; Onozawa-Komatsuzaki, N.; Miyazawa, S.; Sugihara, H.; Hirose, T.; Kasuga, K. pH-Dependent catalytic activity and chemoselectivity in transfer hydrogenation catalyzed by iridium complex with 4,4'-dihydroxy-2,2'-bipyridine. *Chem. - Eur. J.* **2008**, 14 (35), 11076–11081.

(20) Takale, B. S.; Feng, X.; Lu, Y.; Bao, M.; Jin, T.; Minato, T.; Yamamoto, Y. Unsupported Nanoporous Gold Catalyst for Chemoselective Hydrogenation Reactions under Low Pressure: Effect of Residual Silver on the Reaction. *J. Am. Chem. Soc.* **2016**, 138 (32), 10356–10364.

(21) Reis, P. M.; Royo, B. Chemoselective hydrogenation of nitroarenes and deoxygenation of pyridine N-oxides with H₂ catalyzed by MoO₂Cl₂. *Tetrahedron Lett.* **2009**, 50 (8), 949–952.

(22) Suntrup, L.; Hohloch, S.; Sarkar, B. Expanding the Scope of Chelating Triazolylenes: Mesoionic Carbenes from the 1,5-“Click”-Regioisomer and Catalytic Synthesis of Secondary Amines from Nitroarenes. *Chem. - Eur. J.* **2016**, 22 (50), 18009–18018.

(23) Sabater, S.; Müller-Bunz, H.; Albrecht, M. Carboxylate-Functionalized Mesoionic Carbene Precursors: Decarboxylation, Ruthenium Bonding, and Catalytic Activity in Hydrogen Transfer Reactions. *Organometallics* **2016**, 35 (13), 2256–2266.

(24) Sorribes, I.; Wienhöfer, G.; Vicent, C.; Junge, K.; Llusar, R.; Beller, M. Chemoselective transfer hydrogenation to nitroarenes mediated by cubane-type Mo₃S₄ cluster catalysts. *Angew. Chem., Int. Ed.* **2012**, 51 (31), 7794–7798.

(25) Shegavi, M. L.; Bose, S. K. Recent advances in the catalytic hydroboration of carbonyl compounds. *Catal. Sci. Technol.* **2019**, 9 (13), 3307–3336.

(26) Wei, Y.; Liu, S.-X.; Mueller-Bunz, H.; Albrecht, M. Synthesis of Triazolyldiene Nickel Complexes and Their Catalytic Application in Selective Aldehyde Hydrosilylation. *ACS Catal.* **2016**, 6 (12), 8192–8200.

(27) Zheng, J.; Misal Castro, L. C.; Roisnel, T.; Darcel, C.; Sortais, J.-B. Iron piano-stool phosphine complexes for catalytic hydrosilylation reaction. *Inorg. Chim. Acta* **2012**, 380, 301–307.

(28) Johnson, C.; Albrecht, M. Triazolyldiene Iron(II) Piano-Stool Complexes: Synthesis and Catalytic Hydrosilylation of Carbonyl Compounds. *Organometallics* **2017**, 36 (15), 2902–2913.

(29) Licini, G.; Conte, V.; Coletti, A.; Mba, M.; Zonta, C. Recent advances in vanadium catalyzed oxygen transfer reactions. *Coord. Chem. Rev.* **2011**, 255 (19–20), 2345–2357.

(30) Holm, R. H. Metal-centered oxygen atom transfer reactions. *Chem. Rev.* **1987**, 87 (6), 1401–1449.

(31) Xiao, J.; Li, X. Gold α -oxo carbenoids in catalysis: catalytic oxygen-atom transfer to alkynes. *Angew. Chem., Int. Ed.* **2011**, 50 (32), 7226–7236.

(32) Chantarojsiri, T.; Sun, Y.; Long, J. R.; Chang, C. J. Water-Soluble Iron(IV)-Oxo Complexes Supported by Pentapyridine Ligands: Axial Ligand Effects on Hydrogen Atom and Oxygen Atom Transfer Reactivity. *Inorg. Chem.* **2015**, 54 (12), 5879–5887.

(33) Weisser, F.; Stevens, H.; Klein, J.; van der Meer, M.; Hohloch, S.; Sarkar, B. Tailoring Ru(II) pyridine/triazole oxygenation catalysts and using photoreactivity to probe their electronic properties. *Chem. - Eur. J.* **2015**, 21 (24), 8926–8938.

(34) Tonks, I. A. Organometallic mechanisms: Measuring up with the early metals. *Nat. Chem.* **2017**, 9 (9), 834–836.

(35) Schindler, T.; Sauer, A.; Spaniol, T. P.; Okuda, J. Oxygen Atom Transfer Reactions with Molybdenum Cofactor Model Complexes That Contain a Tetradentate OSSO-Type Bis(phenolato) Ligand. *Organometallics* **2018**, 37 (23), 4336–4340.

(36) Beaumier, E. P.; Pearce, A. J.; See, X. Y.; Tonks, I. A. Modern applications of low-valent early transition metals in synthesis and catalysis. *Nat. Rev. Chem.* **2019**, 3 (1), 15–34.

(37) Heinze, K. Bioinspired functional analogs of the active site of molybdenum enzymes: Intermediates and mechanisms. *Coord. Chem. Rev.* **2015**, 300, 121–141.

(38) Schubert, M.; Leppin, J.; Wehming, K.; Schollmeyer, D.; Heinze, K.; Waldvogel, S. R. Powerful fluoroalkoxy molybdenum(V) reagent for selective oxidative arene coupling reaction. *Angew. Chem., Int. Ed.* **2014**, 53 (9), 2494–2497.

(39) Leppin, J.; Förster, C.; Heinze, K. Molybdenum complex with bulky chelates as a functional model for molybdenum oxidases. *Inorg. Chem.* **2014**, 53 (23), 12416–12427.

(40) Dethlefsen, J. R.; Lupp, D.; Teshome, A.; Nielsen, L. B.; Fristrup, P. Molybdenum-Catalyzed Conversion of Diols and Biomass-Derived Polyols to Alkenes Using Isopropyl Alcohol as Reductant and Solvent. *ACS Catal.* **2015**, 5 (6), 3638–3647.

(41) Asako, S.; Sakae, T.; Murai, M.; Takai, K. Molybdenum-Catalyzed Stereospecific Deoxygenation of Epoxides to Alkenes. *Adv. Synth. Catal.* **2016**, 358 (24), 3966–3970.

(42) Hernández-Ruiz, R.; Sanz, R. Dichlorodioxomolybdenum(VI) Complexes: Useful and Readily Available Catalysts in Organic. *Synthesis* **2018**, 50 (20), 4019–4036.

(43) Robertson, J.; Srivastava, R. S. Mo-catalyzed deoxygenation of epoxides to alkenes. *Mol. Catal.* **2017**, 443, 175–178.

(44) Rubio-Presa, R.; Pedrosa, M. A. R.; Fernández-Rodríguez, M. A.; Arnáiz, F. J.; Sanz, R. Molybdenum-Catalyzed Synthesis of Nitrogenated Polyheterocycles from Nitroarenes and Glycols with Reuse of Waste Reduction Byproduct. *Org. Lett.* **2017**, 19 (19), 5470–5473.

(45) Suárez-Pantiga, S.; Hernández-Ruiz, R.; Virumbrales, C.; Pedrosa, M. R.; Sanz, R. Reductive Molybdenum-Catalyzed Direct Amination of Boronic Acids with Nitro Compounds. *Angew. Chem., Int. Ed.* **2019**, 58 (7), 2129–2133.

(46) Sanz, R.; R. Pedrosa, M. Applications of Dioxomolybdenum(VI) Complexes to Organic Synthesis. *Adv. Org. Synth.* **2013**, 182–266.

(47) Sanz, R.; Pedrosa, M. Applications of Dioxomolybdenum(VI) Complexes to Organic Synthesis. *Curr. Org. Synth.* **2009**, 6 (3), 239–263.

(48) Dragutan, V.; Dragutan, I.; Delaude, L.; Demonceau, A. NHC–Ru complexes—Friendly catalytic tools for manifold chemical transformations. *Coord. Chem. Rev.* **2007**, 251 (5–6), 765–794.

- (49) Flanigan, D. M.; Romanov-Michailidis, F.; White, N. A.; Rovis, T. Organocatalytic Reactions Enabled by N-Heterocyclic Carbenes. *Chem. Rev.* **2015**, *115* (17), 9307–9387.
- (50) Sau, S. C.; Hota, P. K.; Mandal, S. K.; Soleilhavoup, M.; Bertrand, G. Stable abnormal N-heterocyclic carbenes and their applications. *Chem. Soc. Rev.* **2020**, *49* (4), 1233–1252.
- (51) Wang, F.; Liu, L.-j.; Wang, W.; Li, S.; Shi, M. Chiral NHC–metal-based asymmetric catalysis. *Coord. Chem. Rev.* **2012**, *256* (9–10), 804–853.
- (52) Wang, W.; Cui, L.; Sun, P.; Shi, L.; Yue, C.; Li, F. Reusable N-Heterocyclic Carbene Complex Catalysts and Beyond: A Perspective on Recycling Strategies. *Chem. Rev.* **2018**, *118* (19), 9843–9929.
- (53) Peris, E. Smart N-Heterocyclic Carbene Ligands in Catalysis. *Chem. Rev.* **2018**, *118* (19), 9988–10031.
- (54) Hopkinson, M. N.; Richter, C.; Schedler, M.; Glorius, F. An overview of N-heterocyclic carbenes. *Nature* **2014**, *510* (7506), 485–496.
- (55) Herrmann, W. A.; Lobmaier, G. M.; Elison, M. N-heterocyclic carbenes as ligands in high-valent molybdenum and tungsten complexes. *J. Organomet. Chem.* **1996**, *520* (1–2), 231–234.
- (56) Mas-Marzá, E.; Reis, P. M.; Peris, E.; Royo, B. Dioxomolybdenum(VI) complexes containing N-heterocyclic carbenes. *J. Organomet. Chem.* **2006**, *691* (12), 2708–2712.
- (57) Li, S.; Kee, C. W.; Huang, K.-W.; Hor, T. S. A.; Zhao, J. Cyclopentadienyl Molybdenum(II/VI) N-Heterocyclic Carbene Complexes: Synthesis, Structure, and Reactivity under Oxidative Conditions. *Organometallics* **2010**, *29* (8), 1924–1933.
- (58) Li, S.; Wang, Z.; Hor, T. S. A.; Zhao, J. First crystallographic elucidation of a high-valent molybdenum oxo N-heterocyclic carbene complex CpMo(VI)O₂(IBz)₂Mo₆O₁₉. *Dalton Trans.* **2012**, *41* (5), 1454–1456.
- (59) Beerhues, J.; Sen, S.; Schowner, R.; Mate Nagy, G.; Wang, D.; Buchmeiser, M. R. Tailored molybdenum imido alkylidene N-heterocyclic carbene complexes as latent catalysts for the polymerization of dicyclopentadiene. *J. Polym. Sci., Part A: Polym. Chem.* **2017**, *55* (18), 3028–3033.
- (60) Buchmeiser, M. R. Recent Advances in the Regio- and Stereospecific Cyclopolymerization of α,ω -Dienes by Tailored Ruthenium Alkylidenes and Molybdenum Imido Alkylidene N-Heterocyclic Carbene Complexes. *Polym. Rev.* **2017**, *57* (1), 15–30.
- (61) Buchmeiser, M. R.; Sen, S.; Lienert, C.; Widmann, L.; Schowner, R.; Herz, K.; Hauser, P.; Frey, W.; Wang, D. Molybdenum Imido Alkylidene N-Heterocyclic Carbene Complexes: Structure-Productivity Correlations and Mechanistic Insights. *ChemCatChem* **2016**, *8* (16), 2710–2723.
- (62) Buchmeiser, M. R.; Sen, S.; Unold, J.; Frey, W. N-heterocyclic carbene, high oxidation state molybdenum alkylidene complexes: functional-group-tolerant cationic metathesis catalysts. *Angew. Chem., Int. Ed.* **2014**, *53* (35), 9384–9388.
- (63) Elser, I.; Benedikter, M. J.; Schowner, R.; Frey, W.; Wang, D.; Buchmeiser, M. R. Molybdenum Imido Alkylidene N-Heterocyclic Carbene Complexes Containing Pyrrolide Ligands: Access to Catalysts with Sterically Demanding Alkoxides. *Organometallics* **2019**, *38* (12), 2461–2471.
- (64) Herz, K.; Podewitz, M.; Stöhr, L.; Wang, D.; Frey, W.; Liedl, K. R.; Sen, S.; Buchmeiser, M. R. Mechanism of Olefin Metathesis with Neutral and Cationic Molybdenum Imido Alkylidene N-Heterocyclic Carbene Complexes. *J. Am. Chem. Soc.* **2019**, *141* (20), 8264–8276.
- (65) Herz, K.; Unold, J.; Hänle, J.; Schowner, R.; Sen, S.; Frey, W.; Buchmeiser, M. R. Mechanism of the Regio- and Stereoselective Cyclopolymerization of 1,6-Hepta- and 1,7-Octadiynes by High Oxidation State Molybdenum–Imidoalkylidene N-Heterocyclic Carbene Initiators. *Macromolecules* **2015**, *48* (14), 4768–4778.
- (66) Koy, M.; Elser, I.; Meisner, J.; Frey, W.; Wurst, K.; Kästner, J.; Buchmeiser, M. R. High Oxidation State Molybdenum N-Heterocyclic Carbene Alkylidyne Complexes: Synthesis, Mechanistic Studies, and Reactivity. *Chem. - Eur. J.* **2017**, *23* (61), 15484–15490.
- (67) Schowner, R.; Elser, I.; Benedikter, M.; Momin, M.; Frey, W.; Schneck, T.; Stöhr, L.; Buchmeiser, M. R. Origin and Use of Hydroxyl Group Tolerance in Cationic Molybdenum Imido Alkylidene N-Heterocyclic Carbene Catalysts. *Angew. Chem., Int. Ed.* **2020**, *59* (2), 951–958.
- (68) Baltrun, M.; Watt, F. A.; Schoch, R.; Hohloch, S. Dioxo-, Oxo-imido-, and Bis-imido-Molybdenum(VI) Complexes with a Bis-phenolate-NHC Ligand. *Organometallics* **2019**, *38* (19), 3719–3729.
- (69) Baltrun, M.; Watt, F. A.; Schoch, R.; Wölper, C.; Neuba, A. G.; Hohloch, S. A new bis-phenolate mesoionic carbene ligand for early transition metal chemistry. *Dalton Trans.* **2019**, *48* (39), 14611–14625.
- (70) Arnold, P. L.; Casely, I. J.; Turner, Z. R.; Carmichael, C. D. Functionalised saturated-backbone carbene ligands: yttrium and uranyl alkoxy-carbene complexes and bicyclic carbene-alcohol adducts. *Chem. - Eur. J.* **2008**, *14* (33), 10415–10422.
- (71) Liddle, S. T.; Edworthy, I. S.; Arnold, P. L. Anionic tethered N-heterocyclic carbene chemistry. *Chem. Soc. Rev.* **2007**, *36* (11), 1732–1744.
- (72) Liddle, S. T.; Arnold, P. L. Synthesis of Heteroleptic Cerium(III) Anionic Amido-Tethered N-Heterocyclic Carbene Complexes. *Organometallics* **2005**, *24* (11), 2597–2605.
- (73) Jones, N. A.; Liddle, S. T.; Wilson, C.; Arnold, P. L. Titanium(III) Alkoxy-N-heterocyclic Carbenes and a Safe, Low-Cost Route to TiCl₃ (THF)₃. *Organometallics* **2007**, *26* (3), 755–757.
- (74) Arnold, P. L.; Kerr, R. W. F.; Weetman, C.; Docherty, S. R.; Rieb, J.; Cruickshank, F. L.; Wang, K.; Jandl, C.; McMullon, M. W.; Pöthig, A.; Kühn, F. E.; Smith, A. D. Selective and catalytic carbon dioxide and heteroallene activation mediated by cerium N-heterocyclic carbene complexes. *Chem. Sci.* **2018**, *9* (42), 8035–8045.
- (75) Arnold, P. L.; Edworthy, I. S.; Carmichael, C. D.; Blake, A. J.; Wilson, C. Magnesium amido N-heterocyclic carbene complexes. *Dalton Trans.* **2008**, *28*, 3739–3746.
- (76) Dardun, V.; Escomel, L.; Jeanneau, E.; Camp, C. On the alcoholysis of alkyl-aluminum(III) alkoxy-NHC derivatives: reactivity of the Al-carbene Lewis pair versus Al-alkyl. *Dalton Trans.* **2018**, *47* (31), 10429–10433.
- (77) Srivastava, R.; Moneuse, R.; Petit, J.; Pavard, P.-A.; Dardun, V.; Rivat, M.; Schiltz, P.; Solari, M.; Jeanneau, E.; Veyre, L.; Thieuleux, C.; Quadrelli, E. A.; Camp, C. Early/Late Heterobimetallic Tantalum/Rhodium Species Assembled Through a Novel Bifunctional NHC-OH Ligand. *Chem. - Eur. J.* **2018**, *24* (17), 4361–4370.
- (78) Srivastava, R.; Quadrelli, E. A.; Camp, C. Lability of Ta-NHC adducts as a synthetic route towards heterobimetallic Ta/Rh complexes. *Dalton Trans.* **2020**, *49* (10), 3120–3128.
- (79) Taakili, R.; Canac, Y. NHC Core Pincer Ligands Exhibiting Two Anionic Coordinating Extremities. *Molecules* **2020**, *25* (9), 2231.
- (80) Borré, E.; Dahm, G.; Aliprandi, A.; Mauro, M.; Dagorne, S.; Bellemin-Lapponnaz, S. Tridentate Complexes of Group 10 Bearing Bis-Aryloxide N-Heterocyclic Carbene Ligands: Synthesis, Structural, Spectroscopic, and Computational Characterization. *Organometallics* **2014**, *33* (17), 4374–4384.
- (81) Despagne-Ayoub, E.; Henling, L. M.; Labinger, J. A.; Bercaw, J. E. Addition of a phosphine ligand switches an N-heterocyclic carbene-zirconium catalyst from oligomerization to polymerization of 1-hexene. *Dalton Trans.* **2013**, *42* (44), 15544–15547.
- (82) Steffanut, P.; Romain, C.; Dagorne, S.; Bellemin-Lapponnaz, S. N-heterocyclic carbene based zirconium complexes for use in lactones ring opening polymerization. Patent No. WO2012076140A1, June 14, 2012.
- (83) Lohrey, T. D.; Bergman, R. G.; Arnold, J. Oxygen Atom Transfer and Intramolecular Nitrene Transfer in a Rhenium β -Diketiminato Complex. *Inorg. Chem.* **2016**, *55* (22), 11993–12000.
- (84) Locher, J.; Watt, F. A.; Neuba, A. G.; Schoch, R.; Munz, D.; Hohloch, S. Molybdenum(VI) bis-imido Complexes of Dipyrromethene Ligands. *Inorg. Chem.* **2020**, *59*, 9847.
- (85) Pedrosa, M. R.; Escibano, J.; Aguado, R.; Díez, V.; Sanz, R.; Arnáiz, F. J. Dinuclear oxomolybdenum(VI) acetylacetonates: Crystal and molecular structure of Mo₂O₅(acac)₂L₂ (L = D₂O, DMF). *Polyhedron* **2007**, *26* (14), 3695–3702.

- (86) Aguado, R.; Escribano, J.; Pedrosa, M. R.; De Cian, A.; Sanz, R.; Arnáiz, F. J. Binuclear oxomolybdenum(V) chlorides: Molecular structure of $\text{Mo}_2\text{O}_4\text{Cl}_2(\text{DMF})_4$ and $\text{Mo}_2\text{O}_4\text{Cl}_2(\text{bipy})_2\cdot\text{DMF}$. *Polyhedron* **2007**, 26 (14), 3842–3848.
- (87) Lyashenko, G.; Herbst-Irmer, R.; Jancik, V.; Pal, A.; Mösch-Zanetti, N. C. Molybdenum oxo and imido complexes of beta-diketiminato ligands: synthesis and structural aspects. *Inorg. Chem.* **2008**, 47 (1), 113–120.
- (88) Hanauer, K.; Förster, C.; Heinze, K. Redox-Controlled Stabilization of an Open-Shell Intermediate in a Bioinspired Enzyme Model. *Eur. J. Inorg. Chem.* **2018**, 2018 (31), 3537–3547.
- (89) Lincoln, S.; Koch, S. A. Synthesis, structure, and interconversion of polypyrazolylborate complexes of molybdenum(V). *Inorg. Chem.* **1986**, 25 (10), 1594–1602.
- (90) Zwettler, N.; Judmaier, M. E.; Strohmeier, L.; Belaj, F.; Mösch-Zanetti, N. C. Oxygen activation and catalytic aerobic oxidation by $\text{Mo}(\text{IV})/(\text{VI})$ complexes with functionalized iminophenolate ligands. *Dalton transactions (Cambridge, England: 2003)* **2016**, 45 (37), 14549–14560.
- (91) Walter, M. D.; Sofield, C. D.; Booth, C. H.; Andersen, R. A. Spin Equilibria in Monomeric Manganocenes: Solid-State Magnetic and EXAFS Studies. *Organometallics* **2009**, 28 (7), 2005–2019.
- (92) Halbach, R. L.; Nocton, G.; Amaro-Estrada, J. I.; Maron, L.; Booth, C. H.; Andersen, R. A. Understanding the Multiconfigurational Ground and Excited States in Lanthanide Tetrakis Bipyridine Complexes from Experimental and CASSCF Computational Studies. *Inorg. Chem.* **2019**, 58 (18), 12083–12098.
- (93) Booth, C. H.; Walter, M. D.; Kazhdan, D.; Hu, Y.-J.; Lukens, W. W.; Bauer, E. D.; Maron, L.; Eisenstein, O.; Andersen, R. A. Decamethylterbocene complexes of bipyridines and diazabutadienes: multiconfigurational ground states and open-shell singlet formation. *J. Am. Chem. Soc.* **2009**, 131 (18), 6480–6491.
- (94) Booth, C. H.; Kazhdan, D.; Werkema, E. L.; Walter, M. D.; Lukens, W. W.; Bauer, E. D.; Hu, Y.-J.; Maron, L.; Eisenstein, O.; Head-Gordon, M.; Andersen, R. A. Intermediate-valence tautomerism in decamethylterbocene complexes of methyl-substituted bipyridines. *J. Am. Chem. Soc.* **2010**, 132 (49), 17537–17549.
- (95) Booth, C. H.; Walter, M. D.; Daniel, M.; Lukens, W. W.; Andersen, R. A. Self-contained Kondo effect in single molecules. *Phys. Rev. Lett.* **2005**, 95 (26), 267202.
- (96) García, N.; García-García, P.; Fernández-Rodríguez, M. A.; Rubio, R.; Pedrosa, M. R.; Arnáiz, F. J.; Sanz, R. Pinacol as a New Green Reducing Agent: Molybdenum-Catalyzed Chemoselective Reduction of Sulfoxides and Nitroaromatics. *Adv. Synth. Catal.* **2012**, 354 (2–3), 321–327.
- (97) Kimura, K.; Zhuang, J.-H.; Kida, M.; Yamashita, Y.; Sakaguchi, Y. Self-Assembling Polycondensation of 4-Aminobenzaldehyde. Preparation of Star-Like Aggregates of Cone-Shaped Poly-(azomethine) Crystals. *Polym. J.* **2003**, 35 (5), 455–459.
- (98) Tran, R.; Kilyanek, S. M. Deoxydehydration of polyols catalyzed by a molybdenum dioxo-complex supported by a dianionic ONO pincer ligand. *Dalton Trans.* **2019**, 48 (43), 16304–16311.
- (99) Garner, M. E.; Hohloch, S.; Maron, L.; Arnold, J. A New Supporting Ligand in Actinide Chemistry Leads to Reactive Bis(NHC)borate-Supported Thorium Complexes. *Organometallics* **2016**, 35 (17), 2915–2922.
- (100) Garner, M. E.; Parker, B. F.; Hohloch, S.; Bergman, R. G.; Arnold, J. Thorium Metallacycle Facilitates Catalytic Alkyne Hydrophosphination. *J. Am. Chem. Soc.* **2017**, 139 (37), 12935–12938.
- (101) Garner, M. E.; Hohloch, S.; Maron, L.; Arnold, J. Carbon-Nitrogen Bond Cleavage by a Thorium-NHC-bpy Complex. *Angew. Chem., Int. Ed.* **2016**, 55 (44), 13789–13792.
- (102) Chakraborty, J.; Mandal, U.; Ghiviriga, I.; Abboud, K. A.; Veige, A. S. Ammonia Synthesis through Hydrolysis of a Trianionic Pincer Ligand-Supported Molybdenum-Nitride Complex. *Chem. - Eur. J.* **2019**, 25 (62), 14059–14063.